

1 Ubiquitous production of branched glycerol dialkyl glycerol tetraethers (brGDGTs) in
2 global marine environments: a new source indicator for brGDGTs

3 Wenjie Xiao^{1,2}, Yinghui Wang², Shangzhe Zhou², Limin Hu³, Huan Yang⁴, Yunping Xu^{1,2*}

4 ¹Shanghai Engineering Research Center of Hadal Science and Technology, College of Marine
5 Sciences, Shanghai Ocean University, Shanghai 201306, China

6 ²MOE Key Laboratory for Earth Surface Process, College of Urban and Environmental Sciences,
7 Peking University, Beijing 100871, China

8 ³Key Laboratory of Marine Sedimentology and Environmental Geology, First Institute of
9 Oceanography, State Oceanic Administration, Qingdao 266061, China

10 ⁴State Key Laboratory of Biogeology and Environmental Geology, China University of Geosciences,
11 Wuhan 430074, China

12 Corresponding author: Y Xu (ypxu@shou.edu.cn)

13

14 Abstract. Presumed source specificity of branched glycerol dialkyl glycerol tetraethers
15 (brGDGTs) from bacteria thriving in soil/peat and isoprenoid GDGTs (iGDGTs) from
16 aquatic organisms led to the development of several biomarker proxies for
17 biogeochemical cycle and paleoenvironment. However, recent studies reveal that
18 brGDGTs are also produced in aquatic environments besides soils and peat. Here we
19 examined three cores from the Bohai Sea and found distinct difference in brGDGT
20 compositions varying with the distance from the Yellow River mouth. We thus propose
21 an abundance ratio of hexamethylated to pentamethylated brGDGT (IIIa/IIa) to
22 evaluate brGDGT sources. The compiling of globally distributed 1354 marine
23 sediments and 589 soils shows that the IIIa/IIa ratio is generally <0.59 for soils, 0.59–
24 0.92 and >0.92 for marine sediments with and without significant terrestrial inputs,
25 respectively. Such disparity confirms the existence of two sources for brGDGTs, a
26 terrestrial origin with lower IIIa/IIa and a marine origin with higher IIIa/IIa, likely
27 attributed to generally higher pH and the production of brGDGTs in cold deep water in

28 sea. The application of the IIIa/IIa ratio to the East Siberian Arctic Shelf proves it a
29 sensitive source indicator for brGDGTs, which is helpful for accurate estimation of
30 organic carbon source and paleoclimates in marine settings.

31

32 1 Introduction

33 Glycerol dialkyl glycerol tetraethers (GDGTs), membrane lipids of archaea and
34 certain bacteria, are widely distributed in marine and terrestrial environments
35 (Reviewed by Schouten et al., 2013). These lipids have been a focus of attention of
36 organic geochemists for more than ten years because they can provide useful
37 environmental and climatic information such as temperature, soil pH, organic carbon
38 source and microbial community structure (e.g., Schouten et al., 2002; Hopmans et al.,
39 2004; Weijers et al., 2006; Lipp et al., 2008; Kim et al., 2010; Peterse et al., 2012; Zhu
40 et al., 2016). There are generally two types of GDGTs, isoprenoid (iGDGTs) and non-
41 isoprenoid, branched GDGTs (brGDGTs; Fig. 1). The former group is more abundant
42 in aquatic settings and generally thought to be produced by Thaumarchaeota, a specific
43 genetic cluster of the archaea domain (Sinninghe Damsté et al., 2002; Schouten et al.,
44 2008), although Euryarchaeota may be a significant source of iGDGTs in the ocean
45 (e.g., Lincoln et al., 2014). In contrast, the 1,2-di-*O*-alkyl-*sn*-glycerol configuration of
46 brGDGTs was interpreted as an evidence for a bacterial rather than archaeal origin for
47 brGDGTs (Sinninghe Damsté et al., 2000; Weijers et al., 2006). So far, only two species
48 of Acidobacteria were identified to contain one brGDGT with two 13,16-dimethyl
49 octacosanyl moieties (Sinninghe Damsté et al., 2011), which hardly explains high
50 diversity and ubiquitous occurrence of up to 15 brGDGT isomers in environments
51 (Weijers et al., 2007b; De Jonge et al., 2014). Therefore, other biological sources of
52 brGDGTs, although not yet identified, are likely.

53 The source difference between brGDGTs and iGDGTs led researchers to
54 developing a branched and isoprenoid tetraether (BIT) index, expressed as relative
55 abundance of terrestrial-derived brGDGTs to aquatic-derived Thaumarchaeota
56 (Hopmans et al., 2004). Subsequent studies found that the BIT index is specific for soil

57 organic carbon because GDGTs are absent in vegetation (e.g., Walsh et al., 2008;
58 Sparkes et al., 2015). The BIT index is generally higher than 0.9 in soils, but close to 0
59 in marine sediments devoid of terrestrial inputs (Weijers et al., 2006; Weijers et al.,
60 2014). Since its advent, the BIT index has been increasingly used in different
61 environments (e.g., Herfort et al., 2006; Kim et al., 2006; Blaga et al., 2011; Loomis et
62 al., 2011; Wu et al., 2013). Besides the BIT index, Weijers et al. (2007b) found that the
63 number of cyclopentane moieties of brGDGTs, expressed as Cyclization of Branched
64 Tetraethers (CBT), correlated negatively with soil pH, while the number of methyl
65 branches of brGDGTs, expressed as Methylation of Branched Tetraethers (MBT), was
66 dependent on annual mean air temperature (MAT) and to a lesser extent on soil pH. The
67 MBT/CBT proxies were further corroborated by subsequent studies (e.g., Sinninghe
68 Damsté et al., 2008; Peterse et al., 2012; Yang et al., 2014a). Assuming that brGDGTs
69 preserved in marine sediments close to the Congo River outflow were derived from
70 soils in the river catchment, Weijers et al. (2007a) reconstructed large-scale continental
71 temperature changes in tropical Africa that span the past 25,000 years by using the
72 MBT/CBT proxy. Recently, De Jonge et al. (2013) used a tandem high performance
73 liquid chromatography-mass spectrometry (2D HPLC-MS) and identified a series of
74 novel 6-methyl brGDGTs which were previously coeluted with 5-methyl brGDGTs.
75 This finding resulted in the redefinition and recalibration of brGDGTs' indexes (e.g.,
76 De Jonge et al., 2014; Xiao et al., 2015).

77 The premise of all brGDGT-based parameters is their source specificity, i.e.,
78 brGDGTs is only biosynthesized by bacteria thriving in soils and peat. Several studies,
79 however, observed different brGDGT compositions between marine sediments and
80 soils on adjacent lands, supporting in situ production of brGDGTs in marine
81 environments (e.g., Peterse et al., 2009a; Zhu et al., 2011; Liu et al., 2014; Weijers et
82 al., 2014; Zell et al., 2014), analogous to lacustrine settings (e.g., Sinninghe Damsté et
83 al., 2009; Tierney & Russell, 2009; Tierney et al., 2012) and rivers (e.g., Zhu et al.,
84 2011; De Jonge et al., 2015; French et al., 2015; Zell et al., 2015). Peterse et al. (2009)
85 compared the brGDGT distribution in Svalbard soils and nearby fjord sediments, and
86 found that concentrations of brGDGTs (0.01–0.20 µg/g dw) in fjord sediments

87 increased towards the open ocean and the distribution was strikingly different from that
88 in soil. Zhu et al. (2011) examined distributions of GDGTs in surface sediments across
89 a Yangtze River-dominated continental margin, and found evidence for production of
90 brGDGTs in the oxic East China Sea shelf water column and the anoxic
91 sediments/waters of the Lower Yangtze River. At the global scale, Fietz et al. (2012)
92 reported a significant correlation between concentrations of brGDGTs and crenarchaeol
93 ($p < 0.01$; $R^2 = 0.57-0.99$), suggesting that a common or mixed source for brGDGTs
94 and iGDGTs are actually commonplace in lacustrine and marine settings. More recently,
95 Sinninghe Damsté (2016) reported tetraethers in surface sediments from 43 stations in
96 the Berau River delta (Kalimantan, Indonesia), and this result, combined with data from
97 other shelf systems, supported a widespread biosynthesis of brGDGTs in shelf
98 sediments especially at water depth of 50–300 m.

99 River and wind are the most important pathways for transporting terrestrial
100 material into sea. In continental shelf, fluvial discharge is more important because
101 brGDGTs in atmospheric dust are either below the detection level (Hopmans et al., 2004)
102 or present at low abundance (Fietz et al., 2013; Weijers et al., 2014). In the remote ocean
103 where no direct impact from land erosion via rivers takes place, eolian transport and in
104 situ production are major contributors for brGDGTs. Weijers et al. (2014) found that
105 distributions of African dust-derived brGDGTs were similar to those of soils but
106 different from those of distal marine sediments, providing a possibility to distinguish
107 terrestrial vs. marine brGDGTs based on molecular compositions. However, so far no
108 robust molecular indicator is available for estimating source of brGDGTs in marine
109 environments. Considering this, we conduct a detailed study about GDGTs in three
110 cores from the Bohai Sea which are subject to the Yellow River influence to different
111 degree. Our purpose is to evaluate the source discerning capability of different brGDGT
112 parameters, from which the most sensitive parameter is selected and applied for
113 globally distributed marine sediments and soils to test whether it is valid at the global
114 scale. Our study supplies an important step for improving accuracy of brGDGT-derived
115 proxies and better understanding the marine carbon cycle and paleoenvironments.

116

117 2 Material and methods

118 2.1 Study area and sampling

119 The Bohai Sea is a semi-enclosed shallow sea in northern China, extending about
120 550 km from north to south and about 350 km from east to west. Its area is 77,000 km²
121 and the mean depth is 18 m (Hu et al., 2009). The Bohai Strait at the eastern portion is
122 the only passage connecting the Bohai Sea to the outer Yellow Sea. Several rivers,
123 including Yellow River, the second largest river in the world in terms of sediment load
124 (Milliman & Meade, 1983), drain into the Bohai Sea with a total annual runoff of
125 890×10^8 m³. One gravity core of 64 cm long (M1; 37.52°N, 119.32°E) was collected in
126 July 2011, while other two cores were collected in July 2013, namely M3 (38.66°N,
127 119.54°E; 53 cm long) and M7 (39.53°N, 120.46°E; 60 cm long) (Fig. 2). The sites M1,
128 M3 and M7 are located in the south, the center and the north of the Bohai Sea,
129 respectively. The cores were transported to the lab where they were sectioned at 1 or 2
130 cm interval. The age model was established on basis of ²¹⁰Pb and ¹³⁷Cs activity, showing
131 that these cores cover the sedimentation period of less than 100 years (Wu et al., 2013
132 and unpublished data).

133

134 2.2 Lipid extraction and analyses

135 The detailed procedures for lipid extraction and GDGT analyses were described in
136 previous studies (Ding et al., 2015; Xiao et al., 2015). Briefly, the homogenous freeze-
137 dried samples were ultrasonically extracted with dichloromethane (DCM)/methanol
138 (3:1 v:v). The extracts were separated into nonpolar and polar fraction over silica gel
139 columns. The latter fraction containing GDGTs was analyzed using an Agilent 1200
140 HPLC-atmospheric pressure chemical ionization-triple quadruple mass spectrometry
141 (HPLC-APCI-MS) system. The separation of 5- and 6-methyl brGDGTs was achieved
142 with two silica columns in sequence (150 mm×2.1 mm; 1.9 μm, Thermo Finnigan;
143 USA). The quantification was achieved by comparison of the respective protonated ion
144 peak areas of each GDGT to the internal standard (C₄₆ GDGT) in selected ion
145 monitoring (SIM) mode. The protonated ions were m/z 1050, 1048, 1046, 1036, 1034,

146 1032, 1022, 1020, 1018 for brGDGTs, 1302, 1300, 1298, 1296, 1292 for iGDGTs and
147 744 for C₄₆ GDGT.

148

149 2.3 Parameter calculation and statistics

150 The BIT, MBT, Methyl Index (MI), Degree of Cyclization (DC) of brGDGTs and
151 weighted average number of cyclopentane moieties for tetramethylated brGDGTs
152 (#Rings_{tetra}) were calculated according to the definitions of Hopmans et al. (2004),
153 Weijers et al. (2007b), Zhang et al. (2011), Sinninghe Damsté et al. (2009) and
154 Sinninghe Damsté (2016), respectively.

$$155 \text{ BIT} = \frac{\text{Ia} + \text{IIa} + \text{IIIa}}{\text{Ia} + \text{IIa} + \text{IIIa} + \text{IV}} \quad (1)$$

$$156 \text{ MBT} = \frac{\text{Ia} + \text{Ib} + \text{Ic}}{\text{Ia} + \text{IIa} + \text{IIIa} + \text{Ib} + \text{IIb} + \text{IIIb} + \text{Ic} + \text{IIc} + \text{IIIc}} \quad (2)$$

$$157 \text{ MI} = 4 \times (\text{Ia} + \text{Ib} + \text{Ic}) + 5 \times (\text{IIa} + \text{IIb} + \text{IIc}) + 6 \times (\text{IIIa} + \text{IIIb} + \text{IIIc}) \quad (3)$$

$$158 \text{ DC} = \frac{\text{Ib} + \text{IIb}}{\text{Ia} + \text{IIa} + \text{Ib} + \text{IIb}} \quad (4)$$

$$159 \text{ \#Rings}_{\text{tetra}} = \frac{\text{Ib} + 2 \times \text{Ic}}{\text{Ia} + \text{Ib} + \text{Ic}} \quad (5)$$

160 where roman numbers denote relative abundance of compounds depicted in Fig. 1. In
161 this study, we used two silica LC columns in tandem and successfully separated 5- and
162 6-methyl brGDGTs. However, many previous studies (e.g., Weijers et al., 2006) used
163 one LC column and did not separate 5- and 6-methyl brGDGTs. Considering this, we
164 combined 5-methyl and 6-methyl brGDGT as one compound in this study, for example,
165 IIIa denotes the total abundance of brGDGT IIIa and IIIa' in figure 1.

166 An analysis of variance (ANOVA) was conducted for different types of samples
167 to determine if they differ significantly from each other. The SPSS 16.0 software
168 package (IBM, USA) was used for the statistical analysis. Squared Pearson correlation
169 coefficients (R²) were reported and a significance level is $p < 0.05$.

170

171 2.4 Data compilation of global soils and marine sediments

172 The dataset in this study are composed of GDGTs from 1354 globally distributed
173 soils and 589 marine sediments (Fig. 2 and supplementary data). These samples span a

174 wide area from 75.00°S to 79.28°N and 168.08°W to 174.40°E and have water depth of
175 1.0 to 5521 m. The marine samples are from the South China Sea (Hu et al., 2012; Jia
176 et al., 2012; O'Brien et al., 2014; Dong et al., 2015), Caribbean Sea (O'Brien et al.,
177 2014), western equatorial Pacific Ocean (O'Brien et al., 2014), southeast Pacific Ocean
178 (Kaiser et al., 2015), the Chukchi and Alaskan Beaufort Seas (Belicka & Harvey, 2009),
179 eastern Indian Ocean (Chen et al., 2014), East Siberian Arctic Shelf (Sparkes et al.,
180 2015), Kara Sea (De Jonge et al., 2015; De Jonge et al., 2016), Svalbard fjord (Peterse
181 et al., 2009a), Red Sea (Trommer et al., 2009), the southern Adriatic Sea (Leider et al.,
182 2010), Columbia estuary (French et al., 2015), globally distributed distal marine
183 sediments (Weijers et al., 2014) and the Bohai Sea (this study). Soil samples are from
184 the Svalbard (Peterse et al., 2009b), Columbia (French et al., 2015), China (Yang et al.,
185 2013; Yang et al., 2014a; Yang et al., 2014b; Ding et al., 2015; Xiao et al., 2015; Hu et
186 al., 2016), globally distributed soils (Weijers et al., 2006; Peterse et al., 2012; De Jonge
187 et al., 2014), California geothermal (Peterse et al., 2009b), France and Brazil (Huguet
188 et al., 2010), western Uganda (Loomis et al., 2011), the USA (Tierney et al., 2012),
189 Tanzania (Coffinet et al., 2014), Indonesian, Vietnamese, Philippine, China and Italia
190 (Mueller-Niggemann et al., 2016).

191

192 3 Results and discussion

193 3.1 Distribution and source of brGDGTs in Bohai Sea

194 A series of iGDGTs including crenarchaea and brGDGTs including 5-methyl and
195 6-methyl isomers were detected in Bohai Sea sediments. For brGDGTs, a total of 15
196 compounds were identified including three tetramethylated brGDGTs (Ia, Ib and Ic),
197 six pentamethylated brGDGTs (IIa, IIb, IIc, IIa', IIb' and IIc') and six hexamethylated
198 brGDGTs (IIIa, IIIb, IIIc, IIIa', IIIb' and IIIc'). In order to evaluate provenances of
199 brGDGTs, we calculated various parameters including the BIT index, percentages of
200 tetra-, penta- and hexa-methylated brGDGTs, #rings for tetramethylated brGDGTs, DC,
201 MI, MBT, brGDGTs IIIa/IIa and Ia/IIa (Table 1). The values of the BIT index ranged
202 from 0.27 to 0.76 in the core M1, which are much higher than that in the core M3 (0.04–
203 0.25) and the core M7 (0.04–0.18). Such difference is expectable since the site M1 is

204 closest to the Yellow River outflow, and receives more terrestrial organic carbon than
205 other two sites (Fig. 2). However, the BIT index itself has no ability to distinguish
206 terrestrial vs. aquatic brGDGTs because brGDGTs and crenarchaea used in this index
207 are thought to be specific for soil organic carbon and marine organic carbon,
208 respectively (Hopmans et al., 2004). For individual brGDGTs, the core M1 is
209 characterized by significantly higher percentage of brGDGT Iia ($28\pm 1\%$) than the core
210 M2 ($18\pm 1\%$) and the core M3 ($18\pm 0\%$; Fig. 3). We performed ANOVA for a variety of
211 brGDGTs' parameters, and the results (Table 1) show that all parameters except MI can
212 distinguish Chinese soils from Bohai Sea sediments, but only the IIIa/Iia ratio can
213 completely separate Chinese soils (0.39 ± 0.25 ; Mean \pm SD; same hereafter), M1
214 sediments (0.63 ± 0.06), M3 sediments (1.16 ± 0.12) and M7 sediments (0.93 ± 0.07) into
215 four groups.

216 Three factors may account for the occurrence of higher IIIa/Iia ratio in the Bohai
217 Sea sediments than Chinese soils: selective degradation during land to sea transport,
218 admixture of river produced brGDGTs and in situ production of brGDGTs in sea.
219 Huguet et al. (2008; 2009) reported that iGDGTs (i.e., crenarchaea) was degraded at a
220 rate of 2-fold higher than soil derived brGDGTs under long term oxygen exposure in
221 the Madeira Abyssal Plain, leading to increase of the BIT index. Such selective
222 degradation, however, cannot explain significant different IIIa/Iia ratio between the
223 Chinese soils and Bohai Sea sediments because unlike crenarchaea, both IIIa and Iia
224 belong to brGDGTs with similar chemical structures and thus have similar degradation
225 rates. In situ production of brGDGTs in rivers is a widespread phenomenon, and can
226 change brGDGTs' composition in sea when they were transported there (e.g., Zhu et al.,
227 2011; De Jonge et al., 2015; Zell et al., 2015). However, this effect is minor in the
228 Yellow River because extremely high turbidity (up to 220 kg/m^3 during the flood season;
229 Ren & Shi, 1986) greatly constrain the growth of aquatic organisms. The studies along
230 lower Yellow River-estuary-coast transect suggested that brGDGTs in surface
231 sediments were primarily a land origin (Wu et al., 2014). Therefore, the enhanced
232 IIIa/Iia values in the Bohai Sea sediments is most likely caused by in situ production of
233 brGDGTs, which is supported by the spatial distributional pattern of IIIa/Iia in the

234 Bohai Sea. The site M1 is adjacent to the Yellow River mouth and receives the largest
235 amount of terrestrial organic matter, causing lower IIIa/IIa values. In contrast, the site
236 M3 located in central Bohai Sea comprises of the least amount of terrestrial organic
237 matter, resulting in higher IIIa/IIa values. The intermediate IIIa/IIa values at the site M7
238 is attributed to moderate land erosion nearby northern Bohai Sea (Fig. 2). These GDGTs'
239 results, consistent with other terrestrial biomarkers such as C₂₉ and C₃₁ *n*-alkanes and
240 C₂₉ sterol (data not showed here), strongly suggest that the IIIa/IIa ratio is a sensitive
241 indicator for assessing source of brGDGTs in the Bohai Sea.

242

243 3.2 Regional and global validation of brGDGT IIIa/IIa

244 To test whether the IIIa/IIa ratio is valid in other environments, we apply it to the
245 Svalbard (Peterse et al., 2009a), the Yenisei River outflow (De Jonge et al., 2015) and
246 the East Siberian Arctic Shelf (Sparkes et al., 2015). By comparing the compositions of
247 brGDGTs in Svalbard soils and nearby fjord sediments, Peterse et al. (2009a) indicated
248 that sedimentary organic matter in fjords was predominantly a marine origin. A plot of
249 BIT vs. IIIa/IIa (Fig. 4a) clearly grouped the samples into two groups which correspond
250 to soils (>0.75 for BIT and <1.0 for IIIa/IIa) and marine sediments (<0.3 for BIT
251 and >1.0 for IIIa/IIa). Another line of evidence is from De Jonge et al. (2015) who
252 examined brGDGTs in core lipids (CLs) and intact polar lipids (IPLs) in the Yenisei
253 River outflow. As the IPLs are rapidly degraded in the environment, they can be used
254 to trace living or recently living material, while the CLs are generated via degradation
255 of the IPLs after cell death (White et al., 1979; Lipp et al., 2008). The compiling of
256 brGDGTs from De Jonge et al. (2015) shows significant difference of the IIIa/IIa ratio
257 between the IPL fractions (>1.0) and CL fractions (<0.8; Fig. 4b). Such disparity
258 supports that brGDGTs produced in marine environments have higher IIIa/IIa values
259 because labile intact polar brGDGTs are mainly produced in situ, whereas recalcitrant
260 core brGDGTs are composed of more allochthonous terrestrial components. Sparkes et
261 al. (2015) examined brGDGTs in surface sediments across the East Siberian Arctic
262 Shelf (ESAS) including the Dmitry-Laptev Strait, Buor-Khaya Bay, ESAS nearshore
263 and ESAS offshore. The plot of BIT vs. IIIa/IIa again results into two groups, one group

264 with lower BIT values (<0.3) and higher IIIa/IIa values (0.8–2.3) mainly from ESAS
265 offshore, and another group with higher BIT values (0.3–1.0) and lower IIIa/IIa values
266 (0.4–0.9) from the Dmitry-Laptev Strait, Buor-Khaya Bay and ESAS nearshore (Fig.
267 4c). A strong linear correlation was observed between the IIIa/IIa ratio and the distance
268 from river mouth ($R^2=0.58$; $p<0.05$; Fig. 4d), in accord with the data of the BIT index
269 and $\delta^{13}\text{C}_{\text{org}}$ (Sparkes et al., 2015). All lines of evidence support that marine-derived
270 brGDGTs have higher IIIa/IIa values than terrestrial derived brGDGTs.

271 We further compile all available data in literatures representing globally
272 distributed soils and marine sediments (Fig. 5). The statistical analysis clearly showed
273 that at the global scale, the IIIa/IIa ratio is significantly higher in marine sediments than
274 soils ($p<0.01$). An exception was observed for Red Sea sediments which have unusually
275 low IIIa/IIa values (0.39 ± 0.21). The Red Sea has a restricted connection to the Indian
276 Ocean via the Bab el Mandeb. This, combined with high insolation, litter precipitation
277 and strong winds result in surface water salinity up to 41 PSU in the south and 36 PSU
278 in the north of the Red Sea (Sofianos et al., 2002). Under such extreme environment,
279 distinct microbial populations may be developed and produced GDGTs different from
280 that in other marine settings (Trommer et al., 2009).

281 Overall, the global distribution of IIIa/IIa presents the highest level in many deep
282 sea sediments (2.6–5.1), the lowest level in soils (<1.0), and an intermediate level in
283 sediments from bays, coastal areas or marginal seas (0.87–2.62; Fig. 5). These results
284 are consistent with our data from the Bohai Sea, and confirm that the IIIa/IIa ratio is a
285 useful proxy for tracing the source of brGDGTs in marine sediments at regional and
286 global scales.

287 Why do marine sediments have higher IIIa/IIa values than soils? It has been
288 reported that relative number of methyl groups positively correlates with soil pH and
289 negatively correlates with MAT (Weijers et al., 2007b; Peterse et al., 2012). The IIIa/IIa
290 ratio is actually an abundance ratio of hexamethylated to pentamethylated brGDGT,
291 and thus is also affected by ambient temperature and pH. Unlike iGDGTs which is well
292 known to be mainly produced by Thaumarchaeota (Sinninghe Damsté et al., 2002;
293 Schouten et al., 2008), the marine source of brGDGTs remains elusive. Here, we assume

294 that marine organisms producing brGDGTs response to ambient temperature in the
295 same way as those soil bacteria producing brGDGTs, i.e., a negative correlation
296 between relative number of methyl group of brGDGTs and ambient temperature.
297 Because a large temperature gradient exists from surface to bottom water in ocean, we
298 need consider the locale where brGDGTs are produced. If brGDGTs in marine
299 environments are predominantly produced in euphotic zone, we would not observe a
300 significant difference for the IIIa/IIa ratio between land and sea because both soils and
301 marine sediments are globally distributed, leading to no systematic difference between
302 soil temperature and sea surface temperature. Alternatively, if brGDGTs in marine
303 sediments are partially derived from deep-water dwelling or benthic organisms, cold
304 deep water (generally 1–2 °C) would cause higher IIIa/IIa values in marine sediments,
305 as we observed in this study. Although to the best of our knowledge, there is no study
306 reporting in situ production of brGDGTs throughout water column in ocean. Recent
307 studies (Taylor et al., 2013; Kim et al., 2015) have suggested that Thaumarchaeota
308 thriving in the deeper, bathypelagic water-column (>1000 m water depth)
309 biosynthesized iGDGTs with different compositions as surface dwelling
310 Thaumarchaeota, and thereby alter signals of TEX₈₆ in sediments. Besides temperature,
311 pH can also alter compositions of brGDGTs (Weijers et al., 2007). Based on global soil
312 data, the IIIa/IIa ratio shows a strong positive correlation with soil pH ($R^2=0.51$; Fig.
313 6). In our study, the majority of soils are acidic or neutral (pH<7.3) and only 8% of soil
314 samples mainly from semi-arid and arid regions have pH of >8.0 (e.g., Yang et al., 2014a).
315 In contrast, seawater is constantly alkaline with a mean pH of 8.2. With this systematic
316 difference, bacteria living in soils tend to produce higher proportions of brGDGT IIa,
317 whereas unknown marine organisms tend to biosynthesize higher proportions of
318 brGDGT IIIa if they response to ambient pH in a similar way as soil bacteria in term of
319 biosynthesis of brGDGTs. It should be pointed out that unlike fairly stable pH of
320 overlying sea water, the pH of pore waters in marine sediments can vary significantly, which
321 may influence compositions of brGDGTs. Nevertheless, at current stage, the occurrence of
322 higher IIIa/IIa values in marine sediments is most likely attributed to relatively higher
323 pH and lower deep water temperature. Further studies are needed to disentangle relative

324 importance of these two factors.

326 3.3 Implication of IIIa/IIa on other brGDGT proxies

327 Because brGDGTs can be produced in marine settings, they are no longer specific
328 for soil organic matter, which inevitably affects brGDGT proxies (e.g., BIT, MBT/CBT).
329 The plot of BIT vs. IIIa/IIa on basis of global dataset shows that the IIIa/IIa ratio has
330 the value of <0.59 for 90% of soil samples and >0.92 for 90% of marine sediments (Fig.
331 7). Considering this fact, we propose that the IIIa/IIa ratio of <0.59 and >0.92 represents
332 terrestrial (or soil) and marine endmembers, respectively. The BIT index has the value
333 of >0.67 for 90% of soils and <0.16 for 90% of marine sediments (Fig. 7). Overall, the
334 BIT index decreased with increasing IIIa/IIa values ($\text{BIT} = 1.08 \times 0.28 \frac{\text{IIIa}}{\text{IIa}} -$
335 0.03 ; $R^2 = 0.77$; Fig. 7), suggesting that both the IIIa/IIa and BIT are useful indexes
336 for assessing soil organic carbon in marine settings. However, when the BIT index has
337 an intermediate value (i.e., 0.16 to 0.67), it is not valid to determine the provenance of
338 brGDGTs. For example, several marine samples having BIT values of ~0.35 show a
339 large range of IIIa/IIa (0.4 to 2.4; Fig. 7), suggesting that the source of brGDGTs can
340 vary case by case. Under this situation, the measurement of the IIIa/IIa ratio is strongly
341 recommended.

342 The different IIIa/IIa values between land and marine endmembers may supply an
343 approach to quantify the contribution of soil organic carbon in marine sediments.
344 Similar to the BIT index, we used a binary mixing model to calculate percentage of soil
345 organic carbon (%OC_{soil}) as follow:

$$346 \quad \%OC_{\text{soil}} = \left[\frac{[\text{IIIa/IIa}]_{\text{sample}} - [\text{IIIa/IIa}]_{\text{marine}}}{[\text{IIIa/IIa}]_{\text{soil}} - [\text{IIIa/IIa}]_{\text{marine}}} \right] * 100 \quad (6)$$

347 Where $[\text{IIIa/IIa}]_{\text{sample}}$, $[\text{IIIa/IIa}]_{\text{soil}}$ and $[\text{IIIa/IIa}]_{\text{marine}}$ are the abundance ratio of brGDGT
348 IIIa/IIa for samples, soils and marine sediments devoid of terrestrial influences,
349 respectively.

350 We applied this binary mixing model to the East Siberian Arctic Shelf because the
351 data of BIT, $\delta^{13}\text{C}_{\text{org}}$ and distance from river mouth are all available (Sparkes et al., 2015).

352 With the distance from river mouth increasing from 25 to >700 km, the BIT, IIIa/IIa
353 and $\delta^{13}\text{C}_{\text{org}}$ change from 0.95 to 0, 0.53 to 2.21 and -27.4‰ to -21.2‰ , respectively,
354 reflecting spatial variability of sedimentary organic carbon sources. For the BIT index,
355 we used 0.97 and 0.01 as terrestrial and marine endmember values based on previous
356 studies for Arctic surrounding regions (De Jonge et al., 2014; Peterse et al., 2014),
357 which are similar to global average values (Hopmans et al., 2004). For $\delta^{13}\text{C}_{\text{org}}$, we chose
358 -27‰ and -20‰ as C3 terrestrial and marine organic carbon endmembers (Meyers,
359 1997). For the IIIa/IIa ratio, we used a global average value of marine sediments (1.6)
360 and soils (0.24), respectively, based on this study. By applying these endmember values
361 into Eq. 6, we calculated percentage of soil organic carbon ($\%\text{OC}_{\text{soil}}$). We removed a
362 few data points if their calculated $\%\text{OC}_{\text{soil}}$ were greater than 100% or below 0%. It
363 should be noted that the endmember value will affect quantitative results, but does not
364 change a general trend of $\%\text{OC}_{\text{soil}}$. The results based on all three parameters show a
365 decreasing trend seawards (Fig. 8). However, the $\%\text{OC}_{\text{soil}}$ based on $\delta^{13}\text{C}_{\text{org}}$ is the highest
366 ($75\pm 18\%$), followed by that from the IIIa/IIa ratio ($58\pm 15\%$) and then that from the BIT
367 index ($43\pm 27\%$). This difference have been explained by that $\delta^{13}\text{C}_{\text{org}}$ is a bulk proxy for
368 marine vs. terrestrial influence of sedimentary organic carbon (SOC), whereas the BIT
369 index is for a portion of the bulk SOC, i.e., soil OC (Walsh et al., 2008) or fluvial OC
370 (Sparkes et al., 2015). For the estimated $\%\text{OC}_{\text{soil}}$, $\delta^{13}\text{C}_{\text{org}}$ presents a stronger positive
371 correlation with the IIIa/IIa ratio ($R^2=0.49$) than the BIT index ($R^2=0.45$), suggesting
372 that the IIIa/IIa ratio may serve a better proxy for quantifying soil organic carbon than
373 the BIT index because it is less affected by selective degradation of branched vs.
374 isoprenoid GDGTs and high production of crenarchaea in marine environments (Smith
375 et al., 2012).

376

377 4 Conclusions

378 Based on a detailed study on GDGTs for three cores in the Bohai Sea and **a**
379 compiling of GDGT data from globally distributed soils and marine sediments, we have
380 reached several important conclusions. Firstly, the ratio of brGDGTs IIIa/IIa is
381 generally lower than 0.59 in soils, but higher than 0.92 in marine sediments devoid of

382 significant terrestrial inputs, making it a sensitive proxy for assessing soil vs. marine
383 derived brGDGTs at regional and global scales. Secondly, in situ production of
384 brGDGTs in marine environments is a ubiquitous phenomenon, which is particularly
385 important for those marine sediments with low BIT index (<0.16) where brGDGTs are
386 exclusively of a marine origin. Thirdly, a systemic difference of the IIIa/IIa value
387 between soils and marine sediments reflects an influence of pH rather than temperature
388 on the biosynthesis of brGDGTs by source organisms. Given these facts, we strongly
389 recommend to calculate the IIIa/IIa ratio before estimating organic carbon source,
390 paleo-soil pH and MAT based on the BIT and MBT/CBT proxies. We also note a
391 relatively large scatter of the IIIa/IIa ratio within both terrestrial and marine realms, and
392 different environmental responses of 5-methyl and 6-methyl brGDGTs (e.g., De Jonge
393 et al., 2014, 2016; Xiao et al., 2015). As a result, the separation of these two types of
394 isomers is needed in future studies to develop more accurate brGDGTs-based proxies.

395

396 *Acknowledgements.* The work was financially supported by the National Science
397 Foundation of China (41476062). We are grateful for X. Dang for GDGT analyses. G.
398 Jia, J. Hu, A. Leider, G. Mollenhauer, G. Trommer and R. Smith are thanked for kindly
399 supplying GDGT data. Dr. Ding He and an anonymous reviewer are thanked for their
400 constructive comments.

401

402 References

- 403 Belicka, L.L., Harvey, H.R., The sequestration of terrestrial organic carbon in Arctic Ocean sediments:
404 A comparison of methods and implications for regional carbon budgets. *Geochim. Cosmochim.*
405 *Acta*, 73, 6231–6248, 2009.
- 406 Blaga, C.I., Reichart, G.J., Vissers, E.W., Lotter, A.F., Anselmetti, F.S., Damste, J.S.S., Seasonal changes
407 in glycerol dialkyl glycerol tetraether concentrations and fluxes in a perialpine lake:
408 Implications for the use of the TEX₈₆ and BIT proxies. *Geochim. Cosmochim. Acta*, 75, 6416–
409 6428, 2011.
- 410 Chen, W., Mohtadi, M., Schefuß, E., Mollenhauer, G., Organic-geochemical proxies of sea surface
411 temperature in surface sediments of the tropical eastern Indian Ocean. *Deep Sea Research Part*

412 I: Oceanographic Research Papers, 88, 17–29, 2014.

413 Coffinet, S., Huguet, A., Williamson, D., Fosse, C., Derenne, S., Potential of GDGTs as a temperature
414 proxy along an altitudinal transect at Mount Rungwe (Tanzania). *Org. Geochem.*, 68, 82–89,
415 2014.

416 De Jonge, C., Hopmans, E.C., Stadnitskaia, A., Rijpstra, W.I.C., Hofland, R., Tegelaar, E., Sinninghe
417 Damsté, J.S., Identification of novel penta- and hexamethylated branched glycerol dialkyl
418 glycerol tetraethers in peat using HPLC–MS2, GC–MS and GC–SMB-MS. *Org. Geochem.*, 54,
419 78–82, 2013.

420 De Jonge, C., Hopmans, E.C., Zell, C.I., Kim, J.-H., Schouten, S., Sinninghe Damsté, J.S., Occurrence
421 and abundance of 6-methyl branched glycerol dialkyl glycerol tetraethers in soils: Implications
422 for palaeoclimate reconstruction. *Geochim. Cosmochim. Acta*, 141, 97–112, 2014.

423 De Jonge, C., Stadnitskaia, A., Cherkashov, G., Sinninghe Damsté, J.S., Branched glycerol dialkyl
424 glycerol tetraethers and crenarchaeol record post-glacial sea level rise and shift in source of
425 terrigenous brGDGTs in the Kara Sea (Arctic Ocean). *Org. Geochem.*, 92, 42–54, 2016.

426 De Jonge, C., Stadnitskaia, A., Hopmans, E.C., Cherkashov, G., Fedotov, A., Streletskaya, I.D., Vasiliev,
427 A.A., Sinninghe Damsté, J.S., Drastic changes in the distribution of branched tetraether lipids
428 in suspended matter and sediments from the Yenisei River and Kara Sea (Siberia): Implications
429 for the use of brGDGT-based proxies in coastal marine sediments. *Geochim. Cosmochim. Acta*,
430 165, 200–225, 2015.

431 Ding, S., Xu, Y., Wang, Y., He, Y., Hou, J., Chen, L., He, J.S., Distribution of branched glycerol dialkyl
432 glycerol tetraethers in surface soils of the Qinghai–Tibetan Plateau: implications of brGDGTs-
433 based proxies in cold and dry regions. *Biogeosciences*, 12, 3141–3151, 2015.

434 Dong, L., Li, Q., Li, L., Zhang, C.L., Glacial–interglacial contrast in MBT/CBT proxies in the South
435 China Sea: Implications for marine production of branched GDGTs and continental
436 teleconnection. *Org. Geochem.*, 79, 74–82, 2015.

437 Fietz, S., Huguet, C., Bendle, J., Escala, M., Gallacher, C., Herfort, L., Jamieson, R., Martínez-García,
438 A., McClymont, E.L., Peck, V.L., Prahl, F.G., Rossi, S., Rueda, G., Sanson-Barrera, A., Rosell-
439 Melé, A., Co-variation of crenarchaeol and branched GDGTs in globally-distributed marine and
440 freshwater sedimentary archives. *Glob. Planet. Change*, 92, 275–285, 2012.

441 Fietz, S., Prahl, F.G., Moraleda, N., Rosell-Melé, A., Eolian transport of glycerol dialkyl glycerol

442 tetraethers (GDGTs) off northwest Africa. *Org. Geochem.*, 64, 112–118, 2013.

443 French, D.W., Huguet, C., Turich, C., Wakeham, S.G., Carlson, L.T., Ingalls, A.E., Spatial distributions
444 of core and intact glycerol dialkyl glycerol tetraethers (GDGTs) in the Columbia River Basin
445 and Willapa Bay, Washington: Insights into origin and implications for the BIT index. *Org.*
446 *Geochem.*, 88, 91–112, 2015.

447 Herfort, L., Schouten, S., Boon, J.P., Woltering, M., Baas, M., Weijers, J.W.H., Damsté, J.S.S.,
448 Characterization of transport and deposition of terrestrial organic matter in the southern North
449 Sea using the BIT index. *Limnol. Oceanogr.*, 51, 2196 - 2205, 2006.

450 Hopmans, E.C., Weijers, J.W.H., Schefuss, E., Herfort, L., Damste, J.S.S., Schouten, S., A novel proxy
451 for terrestrial organic matter in sediments based on branched and isoprenoid tetraether lipids.
452 *Earth Planet. Sci. Lett.*, 224, 107–116, 2004.

453 Hu, J., Meyers, P.A., Chen, G., Peng, P.A., Yang, Q., Archaeal and bacterial glycerol dialkyl glycerol
454 tetraethers in sediments from the Eastern Lau Spreading Center, South Pacific Ocean. *Org.*
455 *Geochem.*, 43, 162–167, 2012.

456 Hu, J., Zhou, H., Peng, P.A., Spiro, B., Seasonal variability in concentrations and fluxes of glycerol
457 dialkyl glycerol tetraethers in Huguangyan Maar Lake, SE China: Implications for the
458 applicability of the MBT–CBT paleotemperature proxy in lacustrine settings. *Chem. Geol.*, 420,
459 200-212, 2016.

460 Hu, L., Guo, Z., Feng, J., Yang, Z., Fang, M., Distributions and sources of bulk organic matter and
461 aliphatic hydrocarbons in surface sediments of the Bohai Sea, China. *Mar. Chem.*, 113, 197–
462 211, 2009.

463 Huguet, A., Fosse, C., Metzger, P., Fritsch, E., Derenne, S., Occurrence and distribution of extractable
464 glycerol dialkyl glycerol tetraethers in podzols. *Org. Geochem.*, 41, 291–301, 2010.

465 Huguet, C., de Lange, G.J., Gustafsson, Ö., Middelburg, J.J., Sinninghe Damsté, J.S., Schouten, S.,
466 Selective preservation of soil organic matter in oxidized marine sediments (Madeira Abyssal
467 Plain). *Geochim. Cosmochim. Acta*, 72, 6061–6068, 2008.

468 Huguet, C., Kim, J.-H., de Lange, G.J., Sinninghe Damsté, J.S., Schouten, S., Effects of long term oxic
469 degradation on the , TEX₈₆ and BIT organic proxies. *Org. Geochem.*, 40, 1188–1194, 2009.

470 Jia, G., Zhang, J., Chen, J., Peng, P.A., Zhang, C.L., Archaeal tetraether lipids record subsurface water
471 temperature in the South China Sea. *Org. Geochem.*, 50, 68–77, 2012.

472 Kaiser, J., Schouten, S., Kilian, R., Arz, H.W., Lamy, F., Sinninghe Damsté, J.S., Isoprenoid and branched
473 GDGT-based proxies for surface sediments from marine, fjord and lake environments in Chile.
474 *Org. Geochem.*, 89, 117–127, 2015.

475 Kim, J.-H., Schouten, S., Rodrigo-Gámiz, M., Rampen, S., Marino, G., Huguet, C., Helmke, P., Buscail,
476 R., Hopmans, E.C., Pross, J., Sangiorgi, F., Middelburg, J.B.M., Sinninghe Damsté, J.S.,
477 Influence of deep-water derived isoprenoid tetraether lipids on the paleothermometer in the
478 Mediterranean Sea. *Geochim. Cosmochim. Acta*, 150, 125-141, 2015.

479 Kim, J.H., Meer, J.V.D., Schouten, S., Helmke, P., Willmott, V., Sangiorgi, F., Koç, N., Hopmans, E.C.,
480 Damsté, J.S.S., New indices and calibrations derived from the distribution of crenarchaeal
481 isoprenoid tetraether lipids: Implications for past sea surface temperature reconstructions.
482 *Geochim. Cosmochim. Acta*, 74, 4639–4654, 2010.

483 Kim, J.H., Schouten, S., Buscail, R., Ludwig, W., Bonnín, J., Sinninghe Damsté, J.S., Bourrin, F., Origin
484 and distribution of terrestrial organic matter in the NW Mediterranean (Gulf of Lions):
485 Exploring the newly developed BIT index. *Geochem. Geophys. Geosy.*, 7, 220–222, 2006.

486 Leider, A., Hinrichs, K.U., Mollenhauer, G., Versteegh, G.J.M., Core-top calibration of the lipid-based
487 UK'37 and TEX₈₆ temperature proxies on the southern Italian shelf (SW Adriatic Sea, Gulf of
488 Taranto). *Earth Planet. Sci. Lett.*, 300, 112–124, 2010.

489 Lincoln, S.A., Wai, B., Eppley, J.M., Church, M.J., Summons, R.E., Delong, E.F., Planktonic
490 Euryarchaeota are a significant source of archaeal tetraether lipids in the ocean. *Proc. Natl. Acad.*
491 *Sci.*, 111, 9858–9863, 2014.

492 Lipp, J.S., Morono, Y., Inagaki, F., Hinrichs, K.U., Significant contribution of Archaea to extant biomass
493 in marine subsurface sediments. *Nature*, 454, 991–994, 2008.

494 Liu, X.-L., Zhu, C., Wakeham, S.G., Hinrichs, K.-U., In situ production of branched glycerol dialkyl
495 glycerol tetraethers in anoxic marine water columns. *Mar. Chem.*, 166, 1–8, 2014.

496 Loomis, S.E., Russell, J.M., Damsté, J.S.S., Distributions of branched GDGTs in soils and lake sediments
497 from western Uganda: Implications for a lacustrine paleothermometer. *Org. Geochem.*, 42, 739–
498 751, 2011.

499 Meyers, P.A., Organic geochemical proxies of paleoceanographic, paleolimnologic, and paleoclimatic
500 processes. *Org. Geochem.*, 27, 213–250, 1997.

501 Milliman, J.D., Meade, R.H., World-wide delivery of river sediment to the oceans. *J. Geol.*, 91, 1-21,

502 1983.

503 Mueller-Niggemann, C., Utami, S.R., Marxen, A., Mangelsdorf, K., Bauersachs, T., Schwark, L.,
504 Distribution of tetraether lipids in agricultural soils—differentiation between paddy and upland
505 management. *Biogeosciences*, 13, 1647–1666, 2016.

506 O’Brien, C.L., Foster, G.L., Martínez-Botí, M.A., Abell, R., Rae, J.W.B., Pancost, R.D., High sea surface
507 temperatures in tropical warm pools during the Pliocene. *Nat Geosci*, 7, 606–611, 2014.

508 Peterse, F., Kim, J.-H., Schouten, S., Kristensen, D.K., Koç, N., Sinninghe Damsté, J.S., Constraints on
509 the application of the MBT/CBT palaeothermometer at high latitude environments (Svalbard,
510 Norway). *Org. Geochem.*, 40, 692–699, 2009a.

511 Peterse, F., Schouten, S., van der Meer, J., van der Meer, M.T.J., Sinninghe Damsté, J.S., Distribution of
512 branched tetraether lipids in geothermally heated soils: Implications for the MBT/CBT
513 temperature proxy. *Org. Geochem.*, 40, 201–205, 2009b.

514 Peterse, F., van der Meer, J., Schouten, S., Weijers, J.W.H., Fierer, N., Jackson, R.B., Kim, J.-H.,
515 Sinninghe Damsté, J.S., Revised calibration of the MBT–CBT paleotemperature proxy based
516 on branched tetraether membrane lipids in surface soils. *Geochim. Cosmochim. Acta*, 96, 215–
517 229, 2012.

518 Peterse, F., Vonk, J.E., Holmes, R.M., Giosan, L., Zimov, N., Eglinton, T.I., Branched glycerol dialkyl
519 glycerol tetraethers in Arctic lake sediments: Sources and implications for paleothermometry at
520 high latitudes. *J. Geophys. Res.-Biogeo.*, 119, 1738–1754, 2014.

521 Ren, M.-E., Shi, Y.-L., Sediment discharge of the Yellow River (China) and its effect on the
522 sedimentation of the Bohai and the Yellow Sea. *Cont. Shelf. Res.*, 6, 785–810, 1986.

523 Schouten, S., Hopmans, E.C., Baas, M., Boumann, H., Standfest, S., Konneke, M., Stahl, D.A.,
524 Sinninghe Damsté, J.S., Intact membrane lipids of "Candidatus Nitrosopumilus maritimus," a
525 cultivated representative of the cosmopolitan mesophilic group I Crenarchaeota. *Appl. Environ.*
526 *Microbiol.*, 74, 2433–2440, 2008.

527 Schouten, S., Hopmans, E.C., Schefuß, E., Sinninghe Damsté, J.S., Distributional variations in marine
528 crenarchaeotal membrane lipids: a new tool for reconstructing ancient sea water temperatures?
529 *Earth Planet. Sci. Lett.*, 204, 265–274, 2002.

530 Schouten, S., Hopmans, E.C., Sinninghe Damsté, J.S., The organic geochemistry of glycerol dialkyl
531 glycerol tetraether lipids: A review. *Org. Geochem.*, 54, 19–61, 2013.

532 Sinninghe Damsté, J.S., Spatial heterogeneity of sources of branched tetraethers in shelf systems: The
533 geochemistry of tetraethers in the Berau River delta (Kalimantan, Indonesia). *Geochim.*
534 *Cosmochim. Acta*, 186, 13–31, 2016.

535 Sinninghe Damsté, J.S., Hopmans, E.C., Pancost, R.D., Schouten, S., Geenevasen, J.A.J., Newly
536 discovered non-isoprenoid glycerol dialkyl glycerol tetraether lipids in sediments. *Chem.*
537 *Commun.*, 17, 1683–1684, 2000.

538 Sinninghe Damsté, J.S., Ossebaar, J., Abbas, B., Schouten, S., Verschuren, D., Fluxes and distribution of
539 tetraether lipids in an equatorial African lake: Constraints on the application of the TEX₈₆
540 palaeothermometer and BIT index in lacustrine settings. *Geochim. Cosmochim. Acta*, 73, 4232–
541 4249, 2009.

542 Sinninghe Damsté, J.S., Ossebaar, J., Schouten, S., Verschuren, D., Altitudinal shifts in the branched
543 tetraether lipid distribution in soil from Mt. Kilimanjaro (Tanzania): Implications for the
544 MBT/CBT continental palaeothermometer. *Org. Geochem.*, 39, 1072-1076, 2008.

545 Sinninghe Damsté, J.S., Rijpstra, W.I.C., Hopmans, E.C., Weijers, J.W.H., Foesel, B.U., Overmann, J.,
546 Dedysh, S.N., 13,16-Dimethyl Octacosanedioic Acid (iso-Diabolic Acid), a Common
547 Membrane-Spanning Lipid of Acidobacteria Subdivisions 1 and 3. *Appl. Environ. Microbiol.*,
548 77, 4147–4154, 2011.

549 Sinninghe Damsté, J.S., Schouten, S., Hopmans, E.C., van Duin, A.C.T., Geenevasen, J.A.J.,
550 Crenarchaeol: the characteristic core glycerol dibiphytanyl glycerol tetraether membrane lipid
551 of cosmopolitan pelagic crenarchaeota. *J. Lipid Res.*, 43, 1641–1651, 2002.

552 Smith, R.W., Bianchi, T.S., Li, X., A re-evaluation of the use of branched GDGTs as terrestrial
553 biomarkers: Implications for the BIT Index. *Geochim. Cosmochim. Acta*, 80, 14-29, 2012.

554 Sofianos, S.S., Johns, W.E., Murray, S.P., Heat and freshwater budgets in the Red Sea from direct
555 observations at Bab el Mandeb. *Deep Sea Res. Part II: Top. Stud. Oceanogr.*, 49, 1323–1340,
556 2002.

557 Sparkes, R.B., Doğrul Selver, A., Bischoff, J., Talbot, H.M., Gustafsson, Ö., Semiletov, I.P., Dudarev,
558 O.V., van Dongen, B.E., GDGT distributions on the East Siberian Arctic Shelf: implications for
559 organic carbon export, burial and degradation. *Biogeosciences*, 12, 3753–3768, 2015.

560 Taylor, K.W.R., Huber, M., Hollis, C.J., Hernandez-Sanchez, M.T., Pancost, R.D., Re-evaluating modern
561 and Palaeogene GDGT distributions: Implications for SST reconstructions. *Glob. Planet.*

562 Change, 108, 158-174, 2013.

563 Tierney, J.E., Russell, J.M., Distributions of branched GDGTs in a tropical lake system: Implications for
564 lacustrine application of the MBT/CBT paleoproxy. *Org. Geochem.*, 40, 1032–1036, 2009.

565 Tierney, J.E., Schouten, S., Pitcher, A., Hopmans, E.C., Sinninghe Damsté, J.S., Core and intact polar
566 glycerol dialkyl glycerol tetraethers (GDGTs) in Sand Pond, Warwick, Rhode Island (USA):
567 Insights into the origin of lacustrine GDGTs. *Geochim. Cosmochim. Acta*, 77, 561–581, 2012.

568 Trommer, G., Siccha, M., Meer, M.T.J.V.D., Schouten, S., Damsté, J.S.S., Schulz, H., Hemleben, C.,
569 Kucera, M., Distribution of Crenarchaeota tetraether membrane lipids in surface sediments from
570 the Red Sea. *Org. Geochem.*, 40, 724–731, 2009.

571 Walsh, E.M., Ingalls, A.E., Keil, R.G., Sources and transport of terrestrial organic matter in Vancouver
572 Island fjords and the Vancouver-Washington Margin: A multiproxy approach using $\delta^{13}\text{C}_{\text{org}}$,
573 lignin phenols, and the ether lipid BIT index. *Limnol. Oceanogr.*, 53, 1054–1063, 2008.

574 Weijers, J.W.H., Schefuß, E., Kim, J.-H., Sinninghe Damsté, J.S., Schouten, S., Constraints on the
575 sources of branched tetraether membrane lipids in distal marine sediments. *Org. Geochem.*, 72,
576 14–22, 2014.

577 Weijers, J.W.H., Schefuß, E., Schouten, S., Damsté, J.S.S., Coupled Thermal and Hydrological Evolution
578 of Tropical Africa over the Last Deglaciation. *Science*, 315, 1701–1704, 2007a.

579 Weijers, J.W.H., Schouten, S., Donker, J.C.V.D., Hopmans, E.C., Damsté, J.S.S., Environmental controls
580 on bacterial tetraether membrane lipid distribution in soils. *Geochim. Cosmochim. Acta*, 71,
581 703–713, 2007b.

582 Weijers, J.W.H., Schouten, S., Spaargaren, O.C., Sinninghe Damsté, J.S., Occurrence and distribution of
583 tetraether membrane lipids in soils: Implications for the use of the TEX_{86} proxy and the BIT
584 index. *Org. Geochem.*, 37, 1680–1693, 2006.

585 White, D.C., Davis, W.M., Nickels, J.S., King, J.D., Bobbie, R.J., Determination of the sedimentary
586 microbial biomass by extractible lipid phosphate. *Oecologia*, 40, 51–62, 1979.

587 Wu, W., Ruan, J., Ding, S., Zhao, L., Xu, Y., Yang, H., Ding, W., Pei, Y., Source and distribution of
588 glycerol dialkyl glycerol tetraethers along lower Yellow River-estuary-coast transect. *Mar.*
589 *Chem.*, 158, 17–26, 2014.

590 Wu, W., Zhao, L., Pei, Y., Ding, W., Yang, H., Xu, Y., Variability of tetraether lipids in Yellow River-
591 dominated continental margin during the past eight decades: Implications for organic matter

592 sources and river channel shifts. *Org. Geochem.*, 60, 33–39, 2013.

593 Xiao, W., Xu, Y., Ding, S., Wang, Y., Zhang, X., Yang, H., Wang, G., Hou, J., Global calibration of a
594 novel, branched GDGT-based soil pH proxy. *Org. Geochem.*, 89, 56–60, 2015.

595 Yang, G., Zhang, C.L., Xie, S., Chen, Z., Gao, M., Ge, Z., Yang, Z., Microbial glycerol dialkyl glycerol
596 tetraethers lipids from water and soil at the Three Gorges Dam on the Yangtze River. *Org.*
597 *Geochem.*, 56, 40–50, 2013.

598 Yang, H., Pancost, R.D., Dang, X., Zhou, X., Evershed, R.P., Xiao, G., Tang, C., Gao, L., Guo, Z., Xie,
599 S., Correlations between microbial tetraether lipids and environmental variables in Chinese soils:
600 Optimizing the paleo-reconstructions in semi-arid and arid regions. *Geochim. Cosmochim. Acta*,
601 126, 49–69, 2014a.

602 Yang, H., Pancost, R.D., Tang, C., Ding, W., Dang, X., Xie, S., Distributions of isoprenoid and branched
603 glycerol dialkanol diethers in Chinese surface soils and a loess–paleosol sequence: Implications
604 for the degradation of tetraether lipids. *Org. Geochem.*, 66, 70–79, 2014b.

605 Zell, C., Kim, J.-H., Dorhout, D., Baas, M., Sinninghe Damsté, J.S., Sources and distributions of
606 branched tetraether lipids and crenarchaeol along the Portuguese continental margin:
607 Implications for the BIT index. *Cont. Shelf. Res.*, 96, 34–44, 2015.

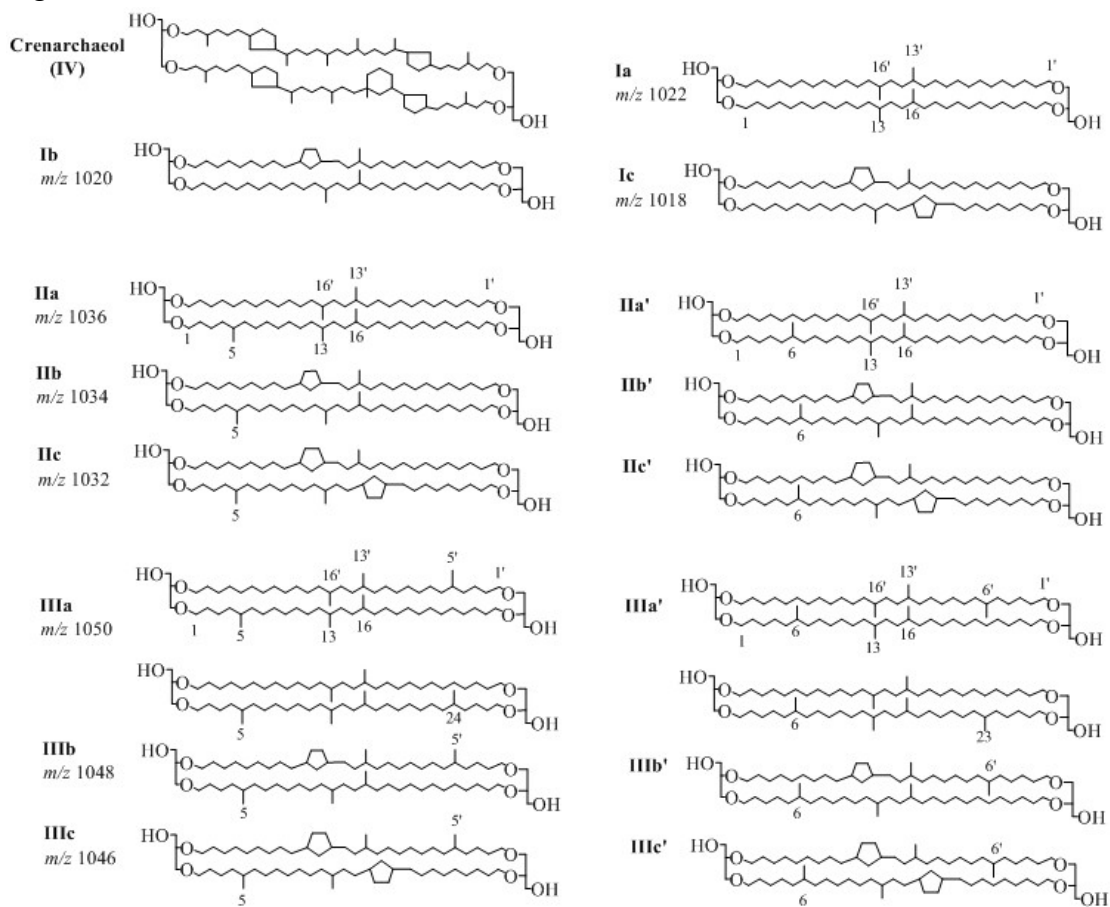
608 Zell, C., Kim, J.-H., Hollander, D., Lorenzoni, L., Baker, P., Silva, C.G., Nittrouer, C., Sinninghe Damsté,
609 J.S., Sources and distributions of branched and isoprenoid tetraether lipids on the Amazon shelf
610 and fan: Implications for the use of GDGT-based proxies in marine sediments. *Geochim.*
611 *Cosmochim. Acta*, 139, 293–312, 2014.

612 Zhang, Y.G., Zhang, C.L., Liu, X.-L., Li, L., Hinrichs, K.-U., Noakes, J.E., Methane Index: A tetraether
613 archaeal lipid biomarker indicator for detecting the instability of marine gas hydrates. *Earth*
614 *Planet. Sci. Lett.*, 307, 525–534, 2011.

615 Zhu, C., Wakeham, S.G., Elling, F.J., Basse, A., Mollenhauer, G., Versteegh, G.J.M., Ouml, nneke, M.,
616 Hinrichs, K.U., Stratification of archaeal membrane lipids in the ocean and implications for
617 adaptation and chemotaxonomy of planktonic archaea. *Environ. Microbiol.*, DOI:
618 10.1111/1462-2920.13289, 2016.

619 Zhu, C., Weijers, J.W.H., Wagner, T., Pan, J.M., Chen, J.F., Pancost, R.D., Sources and distributions of
620 tetraether lipids in surface sediments across a large river-dominated continental margin. *Org.*
621 *Geochem.*, 42, 376–386, 2011.

622 Fig.1. Chemical structures of branched GDGTs and crenarchaeol.



623

624

625

626

627

628

629

630

631

632

633

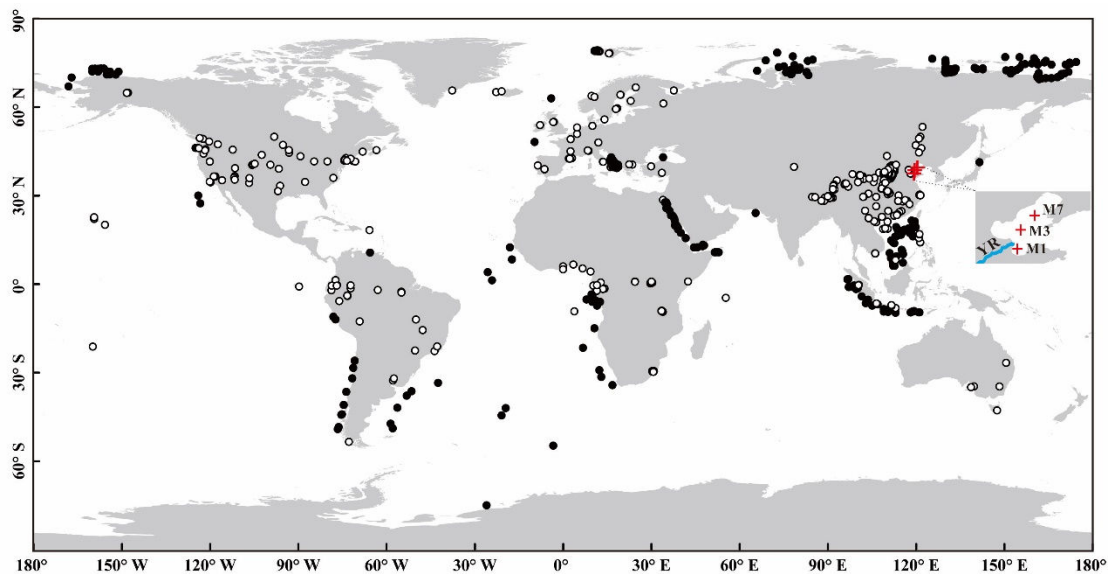
634

635

636

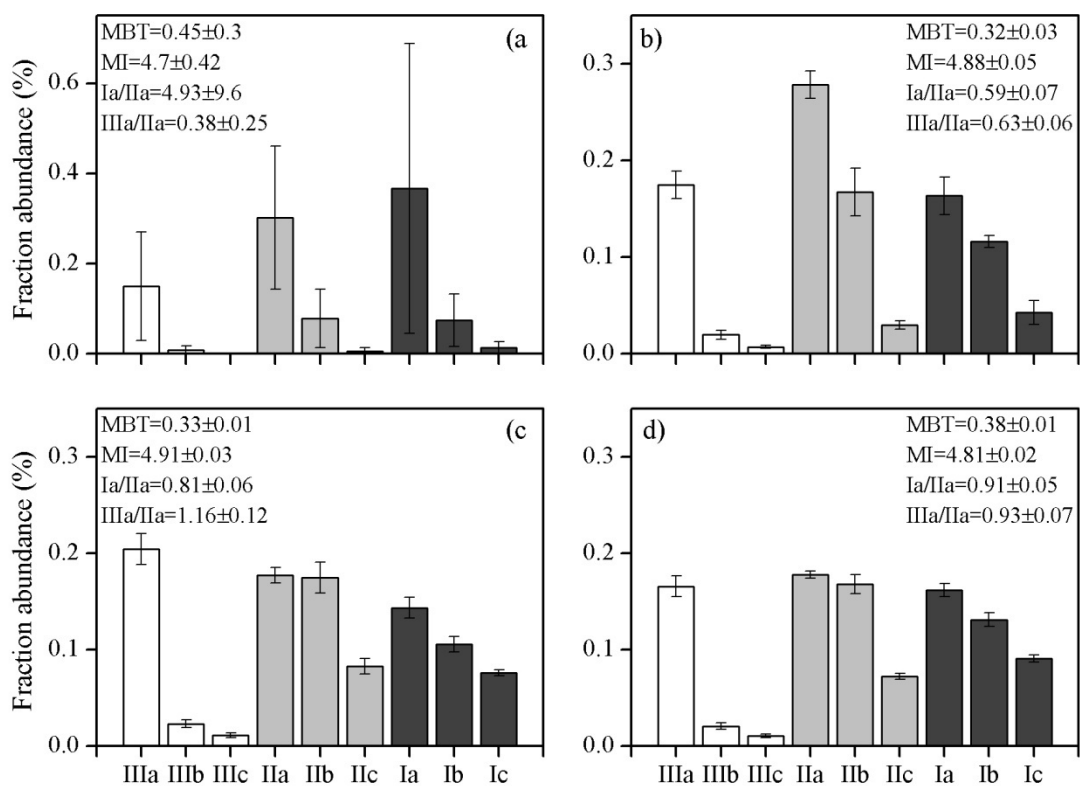
637

638 Fig.2. Location of the samples used in this study. White circles and black circles
639 indicate the soils and marine sediments, respectively. Red crosses denote three sediment
640 cores (M1, M3 and M7) in the Bohai Sea. YR is the Yellow River.



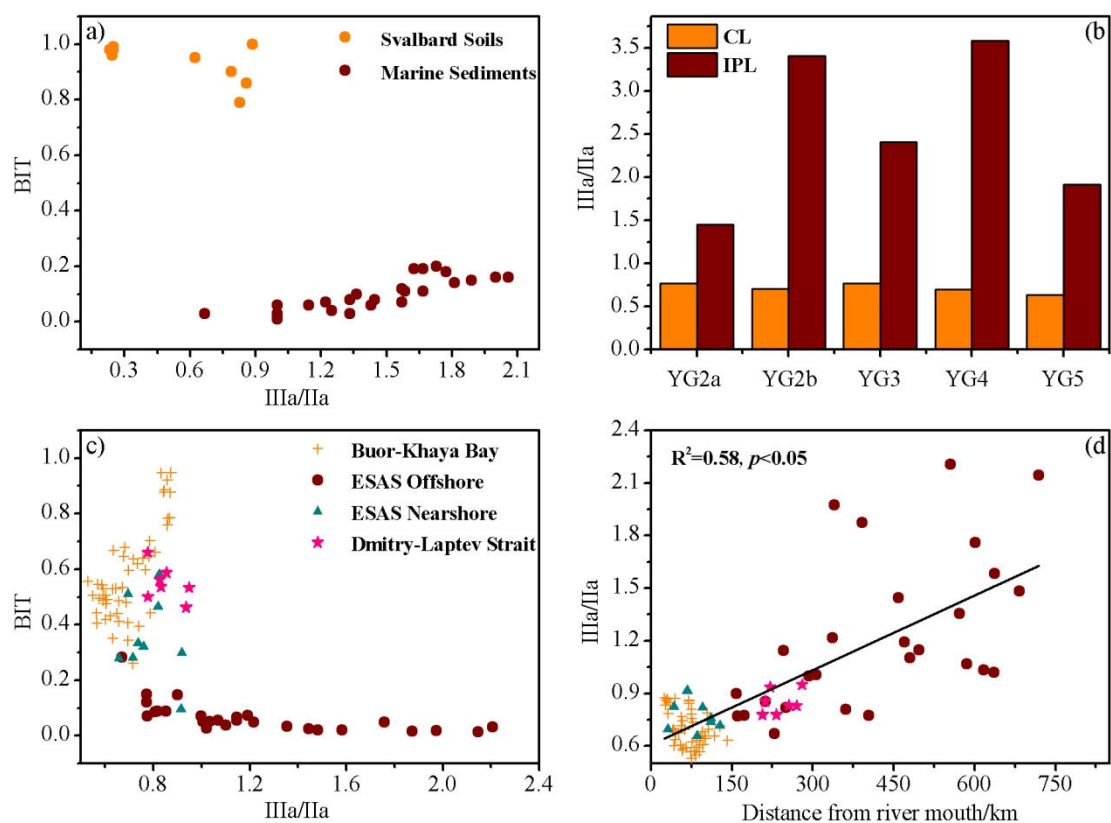
641
642
643
644
645
646
647
648
649
650
651
652
653
654
655
656
657
658

659 Fig.3. Averaged percentages of individual brGDGTs in soils (a), core M1 (b), M3 (c)
 660 and M7 (d). The soil data are from Yang et al. (2014a).



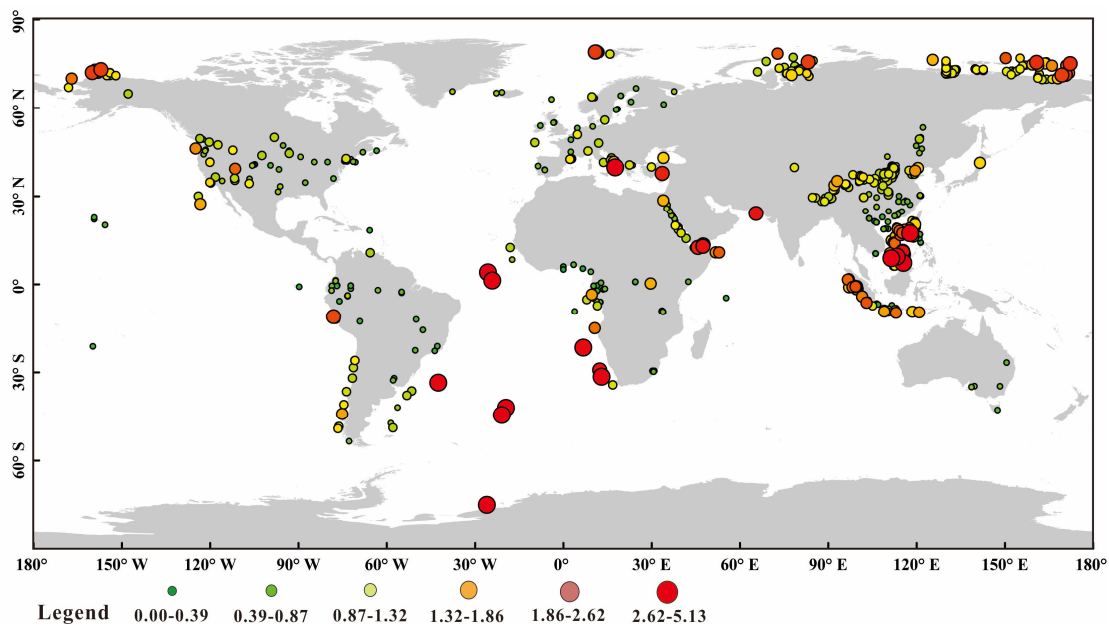
661
 662
 663
 664
 665
 666
 667
 668
 669
 670
 671
 672
 673
 674
 675

676 Fig. 4. a) The relationship between brGDGT IIIa/IIa ratio and the BIT index of samples
 677 from Peterse et al. (2009a); b) histograms of brGDGT IIIa/IIa ratio of the core lipids
 678 (CLs) and intact polar lipids (IPLs) in samples from De Jonge et al. (2015); c) the
 679 relationship between brGDGT IIIa/IIa ratio and the BIT index in samples from Sparkes
 680 et al. (2015); d) the relationship between brGDGT IIIa/IIa ratio and distance from river
 681 mouth in samples from Sparkes et al. (2015).



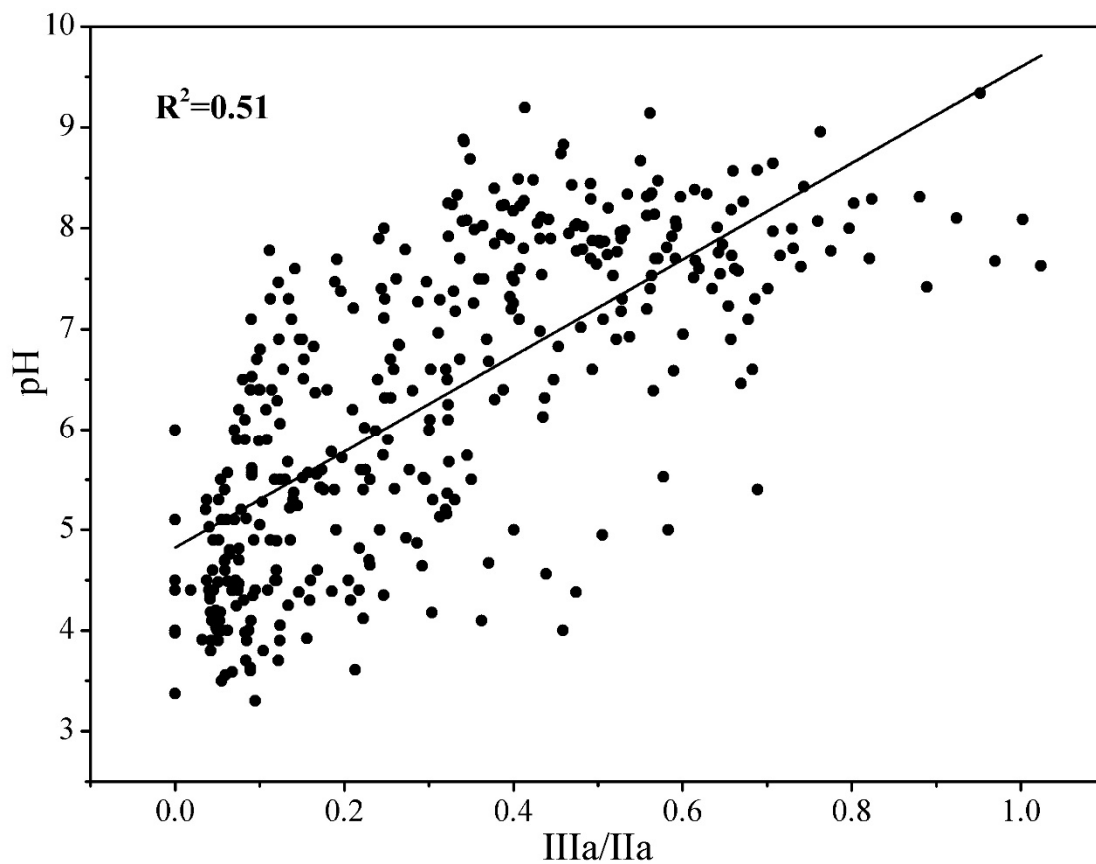
682
 683
 684
 685
 686
 687
 688
 689
 690
 691
 692

693 Fig. 5. Global distribution pattern of brGDGT IIIa/IIa ratio in soils and marine
694 sediments.



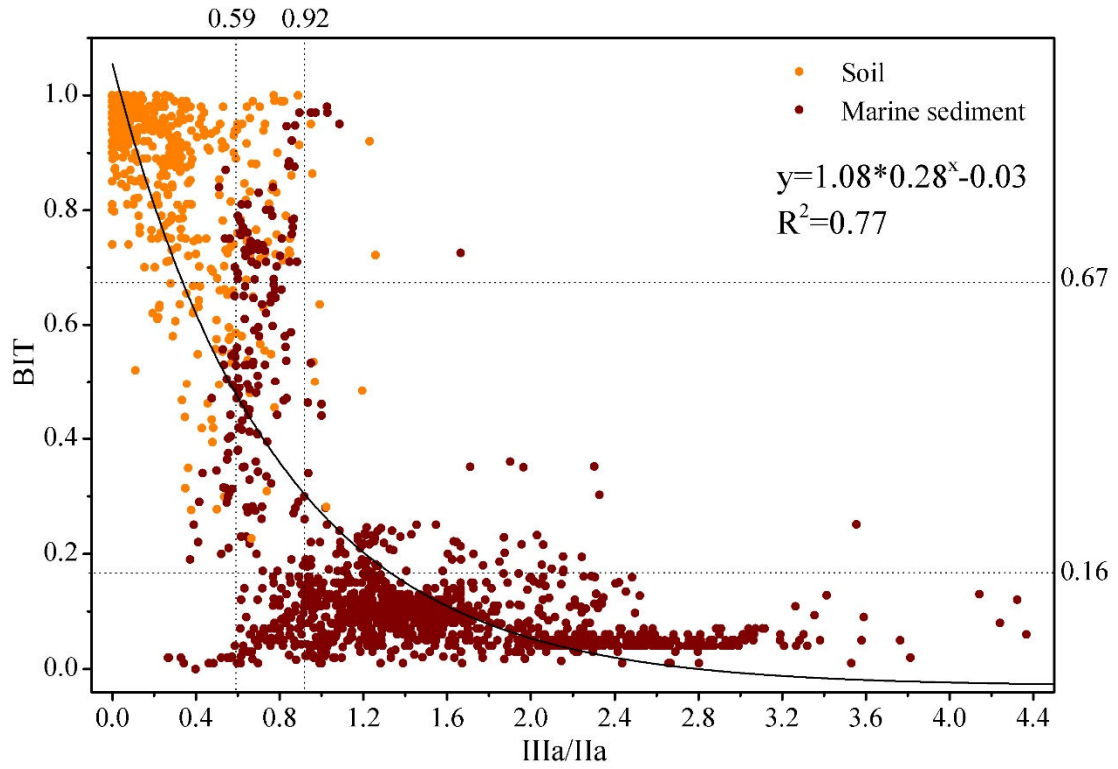
695
696
697
698
699
700
701
702
703
704
705
706
707
708
709
710
711
712
713

714 Fig. 6 a plot showing a positive correlation between soil pH and IIIa/IIa. The data are from
715 Peterse et al. (2012) and this study.



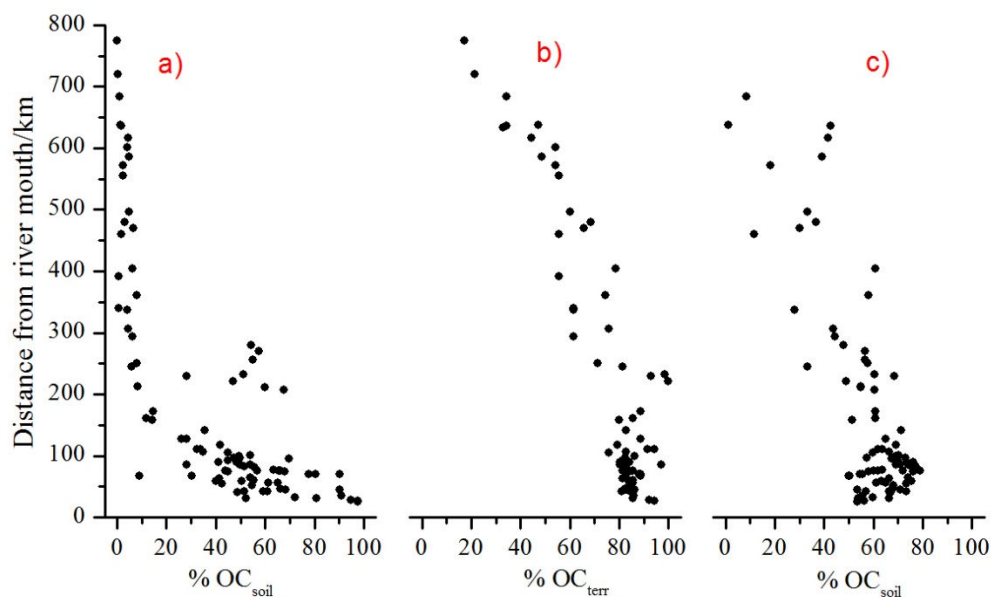
716
717
718
719
720
721
722
723
724
725
726
727
728
729
730

731 Fig. 7. Relationship between the IIIa/IIa ratio and the BIT index of globally distributed
732 samples: soils (orange circle) and marine sediments (red circle). Dashed lines represent
733 lower or upper threshold values for 90% of soils/sediments.



734
735
736
737
738
739
740
741
742
743
744
745
746
747
748

749 Fig. 8. Percentage of soil organic carbon (%OC_{soil}) or terrestrial organic carbon
750 (%OC_{terr}) based on a binary mixing model of BIT (a), $\delta^{13}\text{C}_{\text{org}}$ (b) and IIIa/IIa (c) for the
751 East Siberian Arctic Shelf (Sparkes et al., 2015).



752

753

754

755

756

757

758

759

760

761

762

763

764

765

766

767

768

769

770 Table 1: Parameters including brGDGTs IIIa/IIa, Ia/IIa, the BIT index, MBT, MI, DC,
 771 percentages of tetra-, penta- and hexa-methylated brGDGTs, and the weighted average
 772 number of cyclopentane moieties (#rings for tetramethylated brGDGTs) based on the
 773 GDGTs from three cores (M1, M3 and M7) in the Bohai Sea. Different letters (a, b, c,
 774 d) represent significant difference at the level of $p < 0.05$.

Indexes	Soil	M1	M3	M7
IIIa/IIa	0.39±0.25 (a)	0.63±0.06 (b)	1.16±0.12 (c)	0.93±0.07 (d)
Ia/IIa	4.93±9.60 (a)	0.59±0.07 (b)	0.81±0.06 (b)	0.91±0.05 (b)
BIT	0.75±0.22 (a)	0.50±0.19 (b)	0.14±0.06 (c)	0.11±0.03 (c)
MBT	0.45±0.30 (a)	0.32±0.03 (b)	0.33±0.01 (b)	0.38±0.01 (ab)
MI	4.70±0.42 (a)	4.88±0.05 (b)	4.91±0.03 (b)	4.81±0.02 (ab)
DC	0.31±0.21 (a)	0.62±0.03 (b)	0.79±0.03 (c)	0.82±0.02 (c)
%tetra	0.45±0.30 (a)	0.32±0.03 (b)	0.33±0.01 (c)	0.38±0.01 (c)
%hexa	0.16±0.12 (a)	0.20±0.02 (b)	0.24±0.02 (b)	0.20±0.01 (b)
%penta	0.39±0.20 (a)	0.48±0.02 (b)	0.44±0.02 (b)	0.42±0.01 (b)
#Rings _{Stera}	0.20±0.15 (a)	0.39±0.03 (b)	0.47±0.02 (c)	0.47±0.02 (c)

775

776